Supplement of Biogeosciences, 17, 4477–4487, 2020
https://doi.org/10.5194/bg-17-4477-2020-supplement

Biogeosciences Open Access EGU

Supplement of

Abundance and viability of particle-attached and free-floating bacteria in dusty and nondusty air

Wei Hu et al.

Correspondence to: Daizhou Zhang (dzzhang@pu-kumamoto.ac.jp)

Text S1 Procedure for bacterial enumeration

The particles collected on the filter were transferred into phosphate buffered saline (PBS) in two steps. First, the filter was cut into four pieces and placed in a tube containing 10 mL of PBS. The saline was prefiltered through a 0.025 μm pore filter and autoclaved. The tube was vigorously shaken with a vortex shaker for two minutes. Then, the suspension underwent ultrasonic treatment in ice bath for 15 minutes to detach as many particles from the filter as possible.

The bacterial particles in the suspension were chemically fixed and stained for fluorescence-microscopic counting. The chemical fixation was carried out with 1/25 volume of 25% glutaraldehyde for 30 minutes at 4°C. The fluorescent staining of bacterial particles was performed with the LIVE/DEAD BacLight Bacterial Viability Kit (Invitrogen™, Molecular Probes Inc., Eugene, Oregon). This kit labels bacterial cells with different fluorescent colors according to cell membrane injury; nonviable cells (those with injured membranes) were stained red, and viable cells (those without membrane injuries) were stained green (Fig. S3). The applicability of the fluorescent staining kit to airborne bacteria was introduced in Murata and Zhang (2013).

To make a slide for microscopic counting, the particles in the treated suspension were filtrated and condensed on a black polycarbonate filter (25 mm diameter and 0.2 μm pore size, Advantec®, Toyo Toshi Kaisha, Ltd., Japan). The filter was placed on a glass slide and covered with a drop of immersion oil and a cover glass. For each slide, we counted viable and nonviable bacterial cells in 20 microscopic fields of 100 μm × 100 μm each with a fluorescence microscope (Eclipse 80i, Nikon Corp., Tokyo, Japan). The bacterial concentration (C) in each size range of the Andersen sampler was calculated using the sum of 20 fields:

$$C_{total} = \frac{(N_{viable} + N_{nonviable}) \times S_{25} \times S_{stage}}{S_{count} \times S_{47} \times V_{air}}$$

$$C_{viable} = \frac{N_{viable} \times S_{25} \times S_{stage}}{S_{count} \times S_{47} \times V_{air}}$$

$$C_{nonviable} = \frac{N_{nonviable} \times S_{25} \times S_{stage}}{S_{count} \times S_{47} \times V_{air}}$$

where N is the number of bacterial cells in 20 fields, S_{count} is the area of 20 fields, S_{25} and S_{47} represent the areas of 25 mm and 47 mm diameter filters, respectively, S_{stage} is the area of each stage plate of the Andersen sampler, and V_{air} is the volume of the sample air. The bacterial concentrations of size-segregated airborne particles were described as $dC/d\log D_p$. The upper limit of the particle size was set to 20 μm because it is difficult for particles larger than 20 μm in aerodynamic diameter to remain airborne (Andreas et al., 1995;Mayol et al., 2014).

The designation of the experiment was modified gradually regarding the results obtained in each year. For the samples collected in 2013 and 2014, we counted bacterial cells only. For the samples collected in 2015, we also counted mineral dust-like particles (insoluble and with irregular shapes) in those collected during the occurrence and disappearance of dust events. In 2016, we counted the mineral dust-like particles and

bacterial cells in all samples. In addition, the probability for the overlapping of bacterial cells and mineral dust-like particles on the membranes for enumeration was quite small (several parts per thousand) and not considered.

Text S2 Resuspension of aerosol particles in Andersen samplers

Bulk aerosol particles were collected on 0.2 μm pore polycarbonate filters (47 mm; Merck Millipore Ltd., Cork, Ireland) using in-line filter holders for 24 hours. Three pairs of aerosol samples were collected during 29–30 May, 16–17 October, and 2–3 November 2014. After collection, one particle-loading filter of each pair was placed on the top stage (Stage 0) plate of the Andersen sampler, and sterilized new filters were set on the plates of stages 1 to 7. The sampler was vacuumed (28.3 L min^{-1}) in a clean hood consistently for sample collection for 24 hours. Then, the filters were treated, and the concentrations of bacterial cells in each stage were enumerated based on the LIVE/DEAD BacLight bacterial viability assay to evaluate the amount of bacteria that fell from the upper stage to the next stage. The results showed that approximately 32% of the bacteria fell from the original filters in stage 0 to lower stages, after which approximately a half (48 ± 15%) of the bacteria were trapped by stage 1 and approximately one fifth (22 ± 9%) of the bacteria were trapped by stage 2 (Figure S5-1). In addition, the estimated total bacterial concentrations of the Andersen sampler were compared with those determined using another holder, and the values were consistent (100±15%) with each other.

The transfer of bacterial cells from stages 4 and 5 (nominally just over 1 μm) to stage 6 (nominally just under 1 μm) was also assessed. Two sets of bulk aerosol particles were collected on 0.2 μm pore polycarbonate filters (47 mm; Merck Millipore Ltd., Cork, Ireland) using in-line holders for 3, 12 and 24 hours, respectively in the indoor environment. One set of three samples were put on the Stage 4 plate of the Andersen sampler, and sterilized new filters were set on the plates of stages 5 to 7. Another set of three samples were put on the Stage 5 plate of the Andersen sampler, respectively, and sterilized new filters were set on the plates of stages 6 to 7. The sampler was vacuumed (28.3 L min^{-1}) in a clean hood consistently for sample collection for 3, 12 and 24 hours correspondingly. After vacuuming, all the filters were treated, and the concentrations of bacterial cells in each stage were enumerated based on the LIVE/DEAD BacLight bacterial viability assay. The results showed that on average less than 10% of the bacteria fell from the original filters in Stage 4 or 5 to lower stages (Fig. S5-2).

The results above suggest that the fractions and concentrations of particle-attached bacteria obtained by the presented method were potentially underestimated. But the underestimation did not significantly affect the size distributions of particle-attached bacteria, and, in particular, the underestimation of the concentrations of particle-attached bacterial cells was less than 10% on average.

To assess whether the detected single-cell bacteria had fallen from the upper stages, we calculated the ideal cell sizes of airborne bacteria collected on the 0.65 μm stage. The 50% cut-off aerodynamic diameter (D_{p50}) was calculated using the following equation:

$$D_{p50} = \sqrt{\frac{18\mu\psi N\pi \cdot Dc^3 \cdot 60}{4CQ\rho}}$$

where μ is the viscosity coefficient of air (1.8×10^{-4} g cm^{-1} s^{-1}), ψ is the inertia parameter (0.14 for 50% impaction efficiency), N is the number (216) of jet nozzles of the stage, D_c is the diameter of each jet nozzle (0.025 cm), C is the Cunningham correlation factor ($1.00 + 0.16 \times 10^{-4}/D_p$), Q is the flow rate (28300 cm^3 min^{-1}), and ρ is the density of the particle. According to the buoyant density of bacterial cells, 1.03–1.24 g cm^{-3} (Bakken and Olsen, 1983;Bratbak and Dundas, 1984), the D_{p50} of the bacterial cells collected in this study was calculated as 0.58–0.64 μm. This size range is consistent with the sizes of cells under microscopic field, although we did not measure the size of all bacterial cells. Hara et al. (2011) previously measured the size distribution of airborne bacterial cells by fluorescence microscopy and image analysis and reported a mode size of approximately 0.6 μm, which is consistent with our results. Additionally, Huffman et al. (2012) detected a peak of fluorescent biological aerosol particles at approximately 0.7 μm and 3 μm using the ultraviolet aerodynamic particle sizer (UV-APS). These results support that a single bacterial cell could be suspended in the air and collected at the lowest stage of the Andersen sampler.

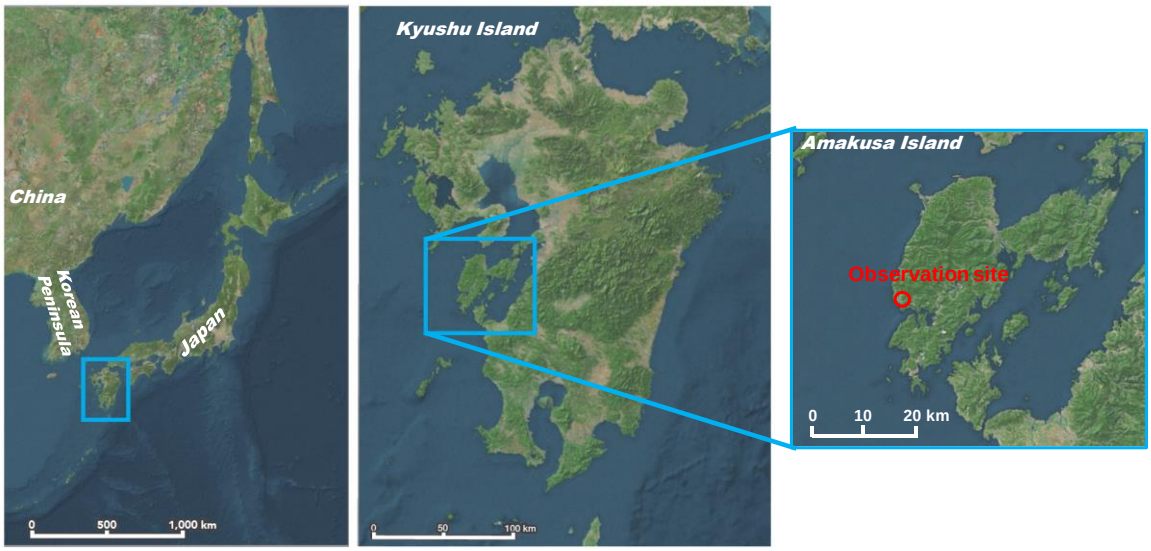

Figure S1. Location of the observation site. The map source is © Google Earth.

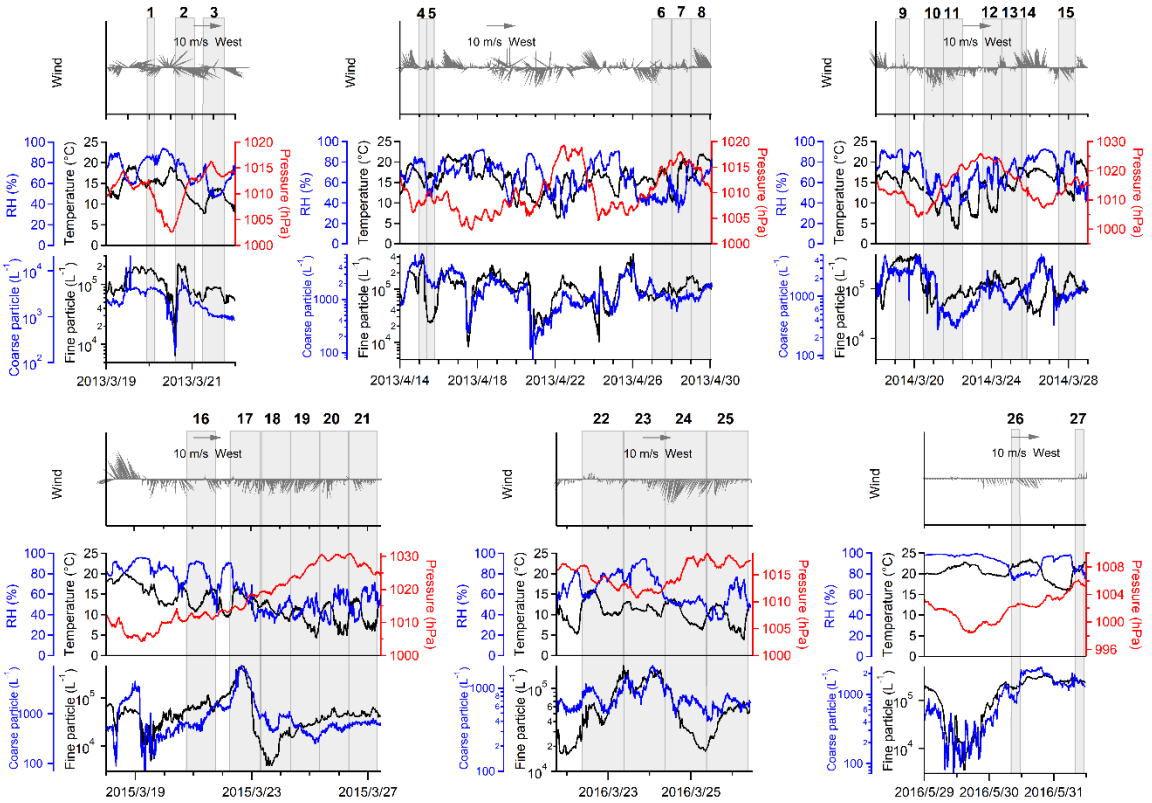

Figure S2. Time series of meteorological conditions and airborne particle number concentrations during the observations. Each sampling period is indicated with a gray shadow and the sequence number.

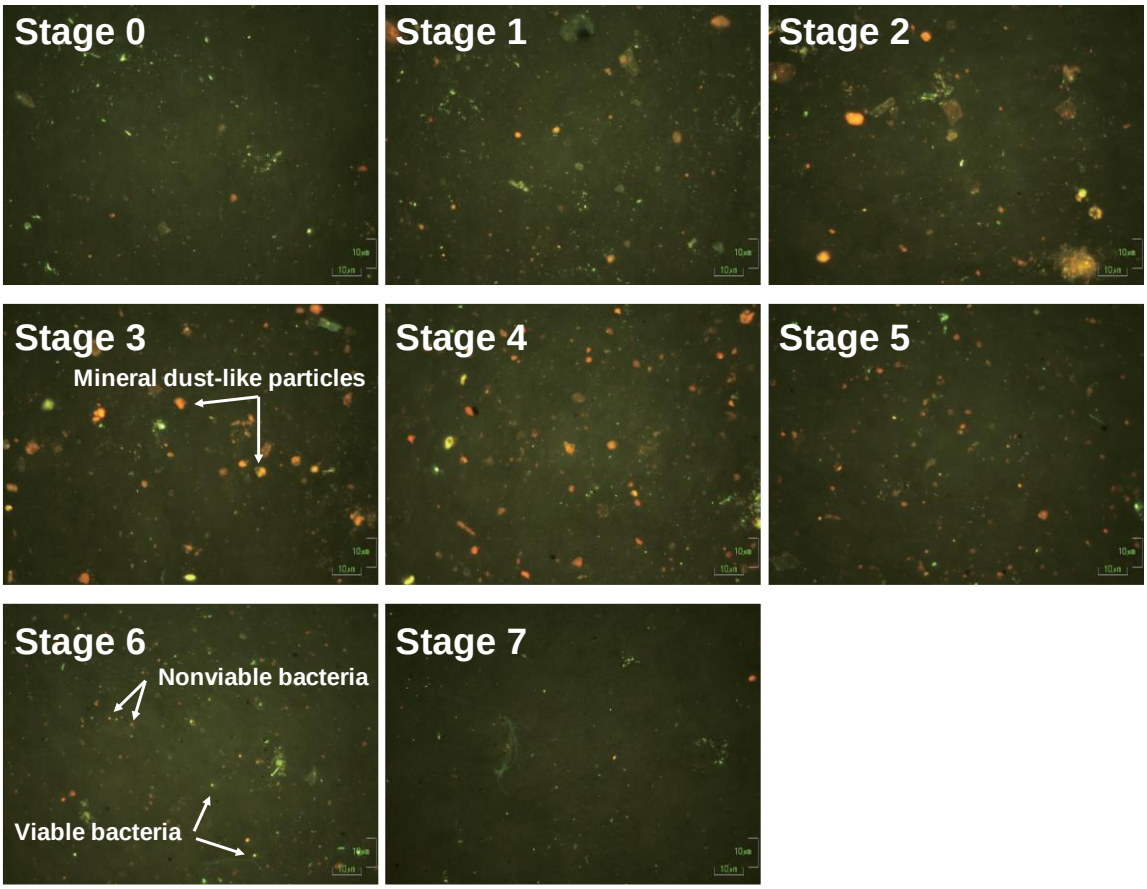

Figure S3. Images of one set of stained samples collected on 20 March 2013 (Sample 2D-Po, dust period) under epifluorescence microscopy field.

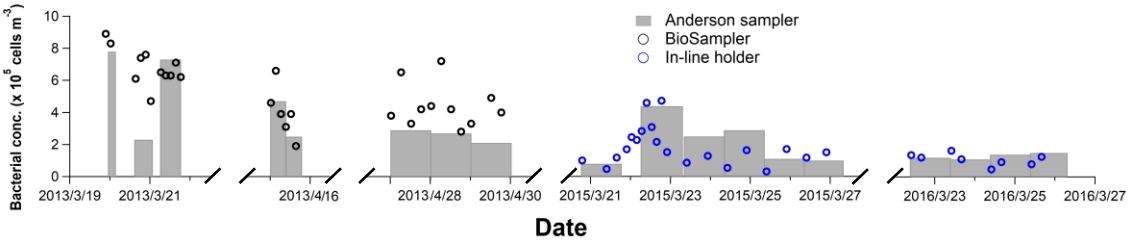

Figure S4. Comparison between the results of the Andersen sampler and the BioSampler (2013) / in-line filter holders (2015–2016). The flow rate for the BioSampler/holder was 10–12.5 L min^{-1}, and the collection duration was 1–2 hours. More details on sample collection with the BioSampler and the in-line filter holder are available in Murata and Zhang (2016) and Hu et al. (2017), respectively. The discrepancy between the results of the Andersen sampler and the other two samplers in some cases might have been caused by the different sampling durations and collection efficiencies of the samplers (e.g., for the Andersen sampler, there was a loss of bacteria due to bouncing, and the size fraction smaller than 0.43 μm was missing).

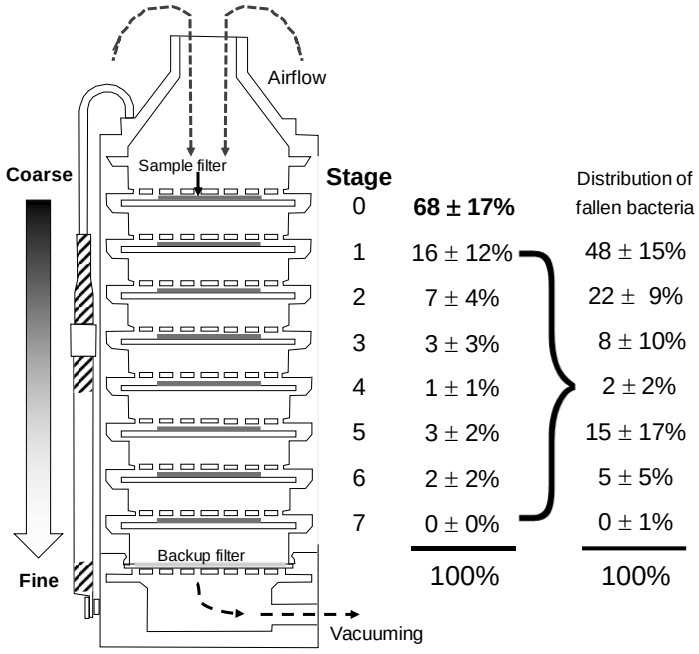

Figure S5-1. Percentages of residual bacterial cells after the sampler was run for 24 h. If no bacteria fall from the top stage, the percentage in bold should be nearly 100%. The actual percentage was 68%, indicating that 32% of the bacteria fell from the top stage. The distribution of fallen bacteria is shown in the right column. The fallen bacteria were mostly in the second and third stages and did not affect the lower stages of the sampler.

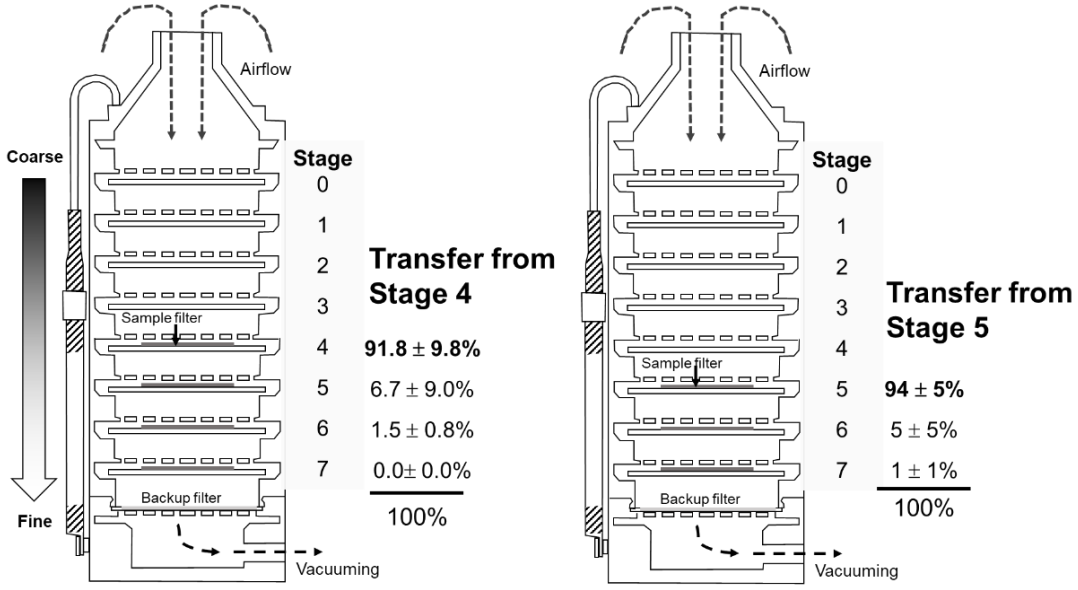

Figure S5-2. The distribution of bacterial cells fallen from Stage 4 (left) and Stage 5 (right) to lower stages. Averagely less than 10% of the bacteria fell from the original filters in Stage 4 or 5 to lower stages.

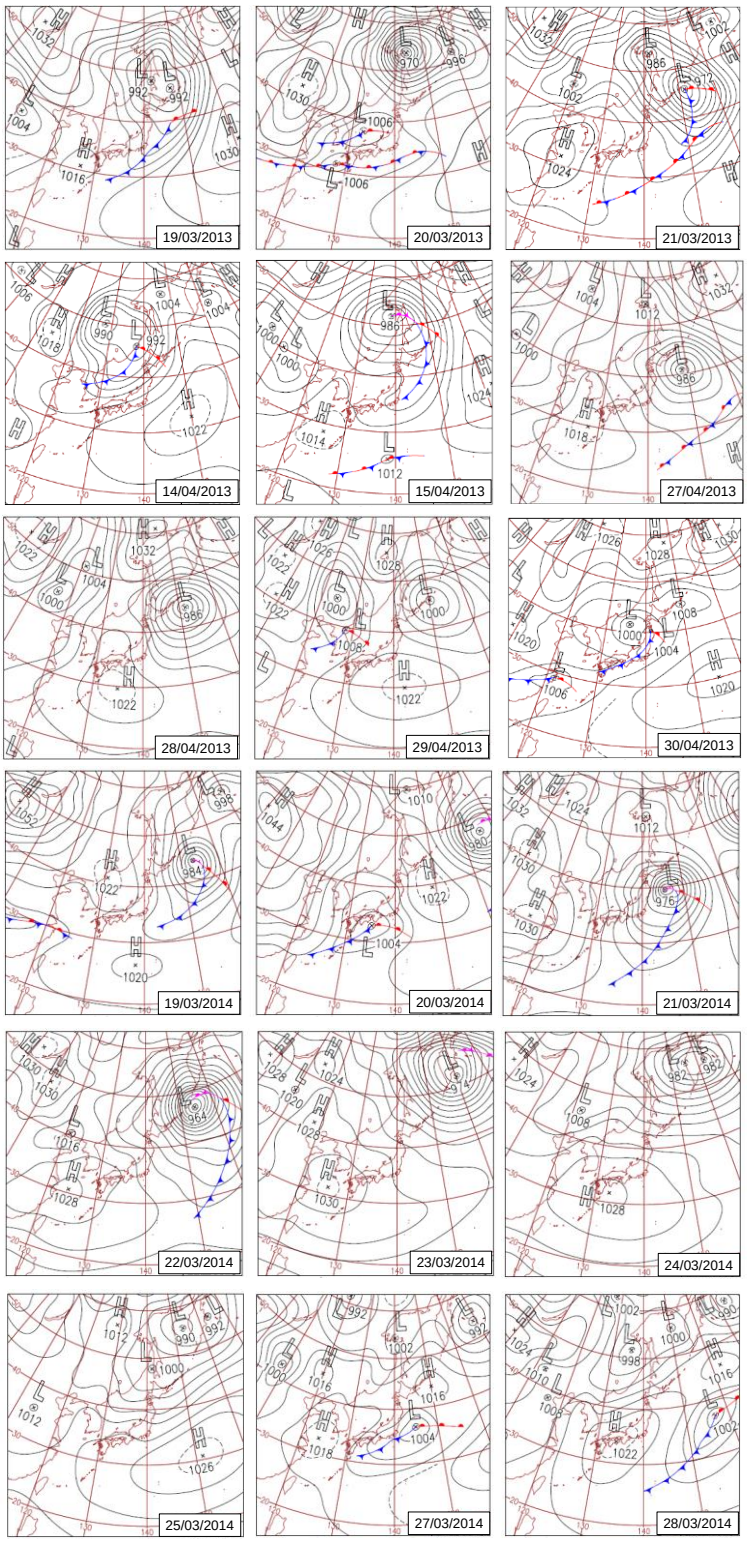

Figure S6-1. Daily weather charts (9:00 am JST every day) during the sampling periods. The data were downloaded from the Japan Meteorological Agency (http://www.data.jma.go.jp/fcd/yoho/hibiten/index.html).

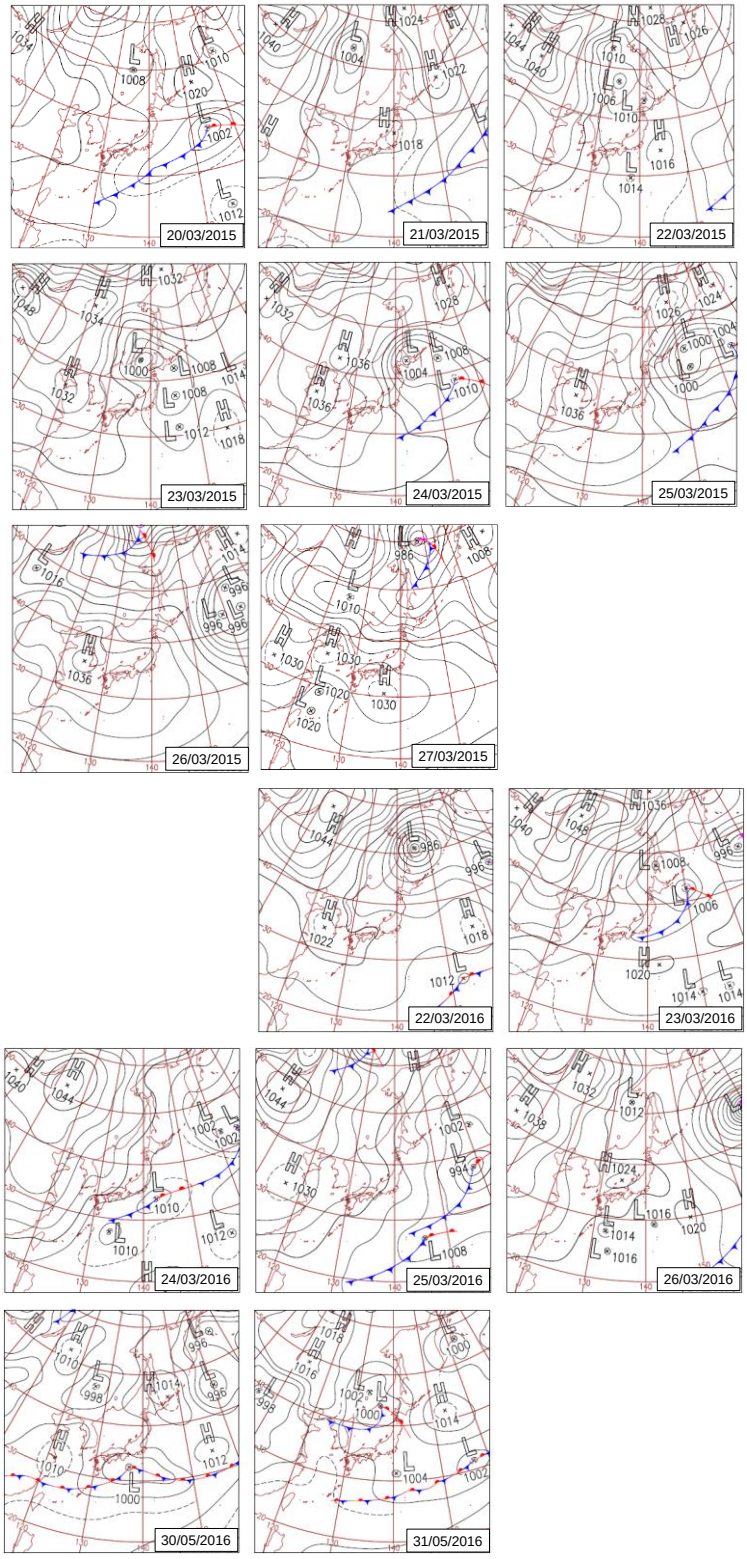

Figure S6-2. Continued.

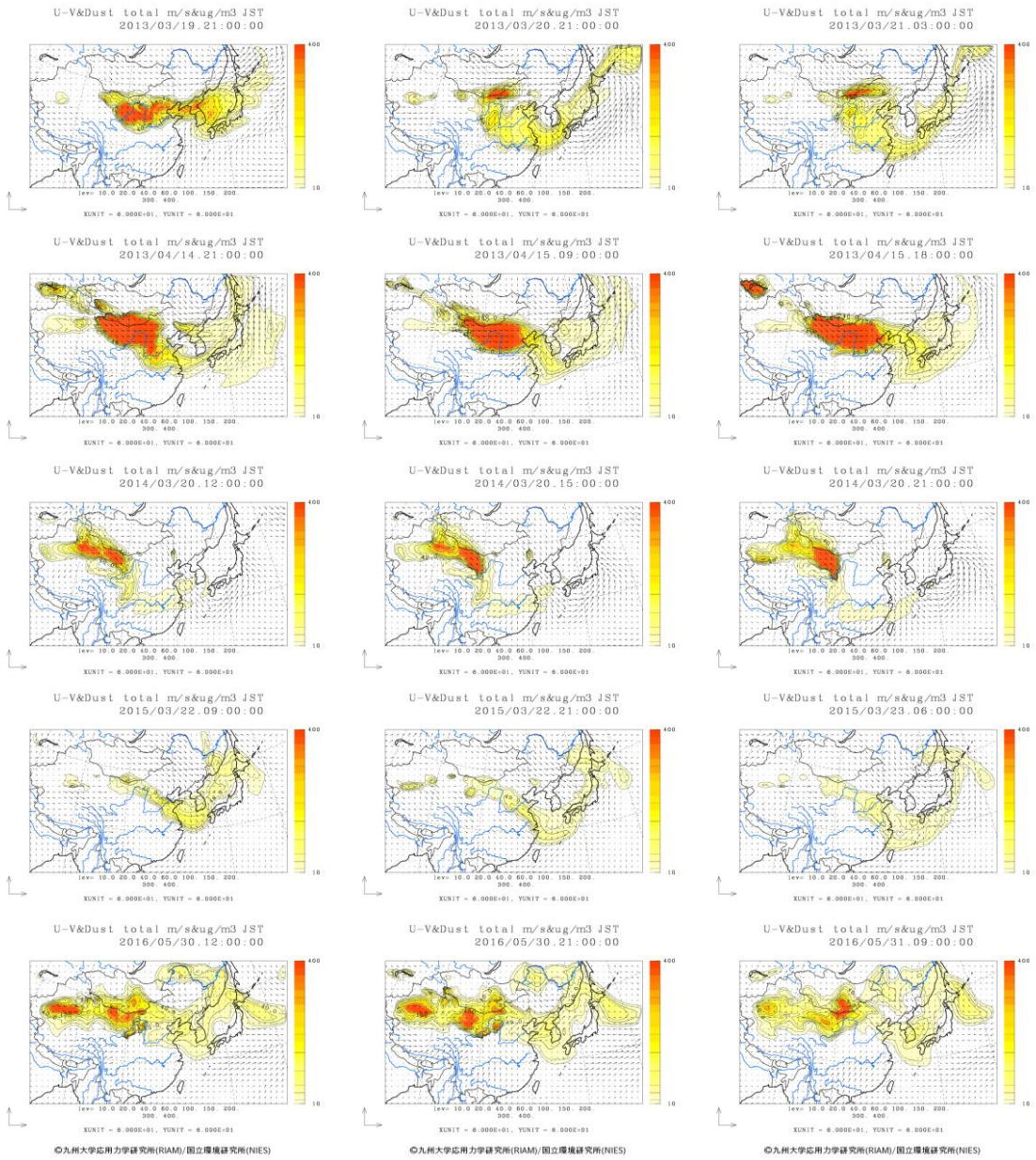

Figure S7. Spatial distributions of Asian dust in the east Asian region during the observed dust events. The data were forecasted by online RIAM/CGER/NIES-CFORS (Chemical weather FORecasting System; http://www-cfors.nies.go.jp/~cfors/).

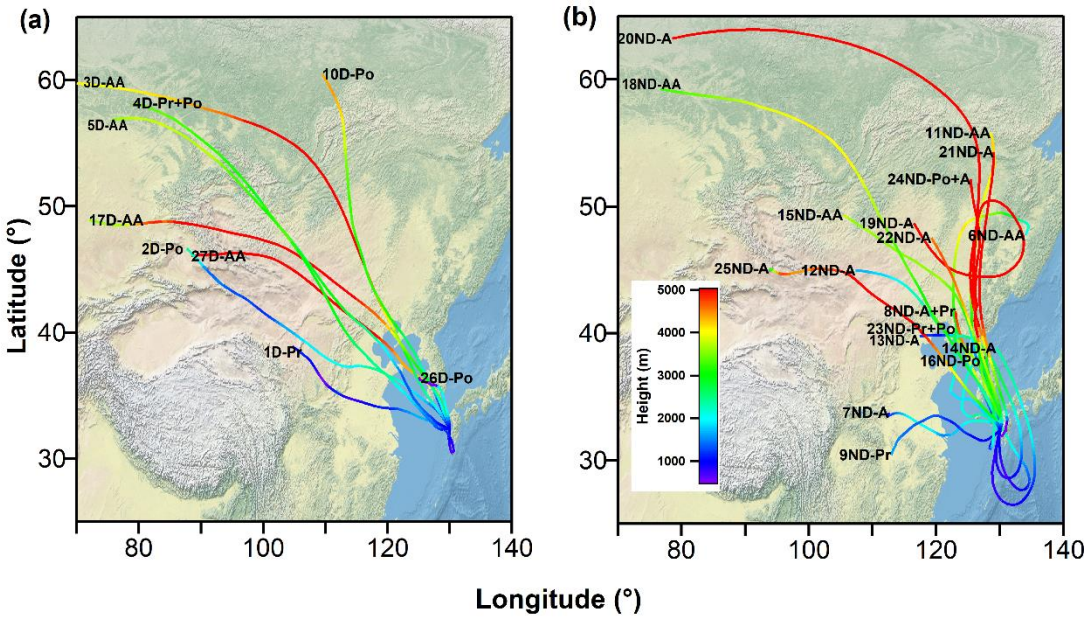

Figure S8. Seventy-two-hour backward trajectories of air parcels (http://ready.arl.noaa.gov/HYSPLIT.php) at 1000 m at the sampling site during the dusty (a) and nondusty (b) periods. The sample ID of each sample is marked at the end of the corresponding trajectory. The map source is the IgorGIS package of IGOR Pro.

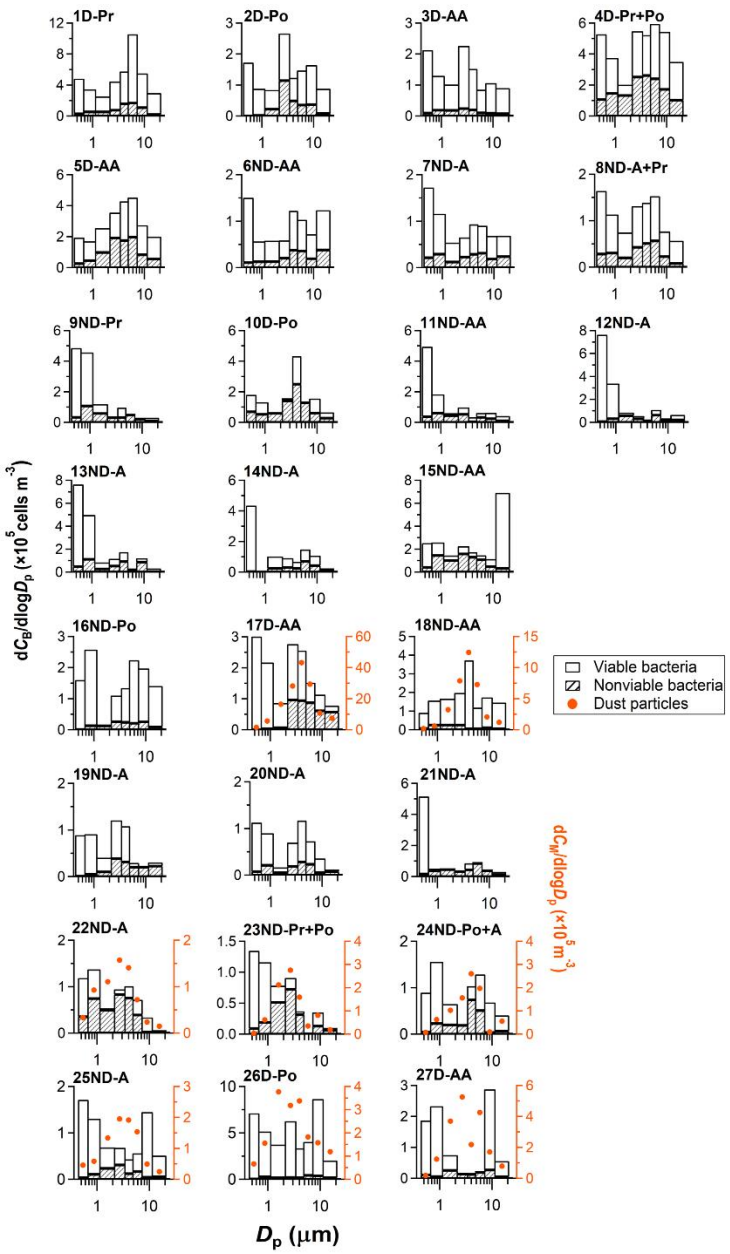

Figure S9. Concentrations of viable and nonviable bacteria (C_B) and mineral dust-like particles (C_M) in size-segregated airborne particles during the sampling periods. All *x* axes indicate particle aerodynamic diameter (D_p), left *y* axes indicate dC_B /dlog D_p (black), and right *y* axes indicate dC_M /dlog D_p (orange). The upper limit of particle size was set to 20 μm because it is difficult for particles larger than 20 μm in aerodynamic diameter to remain airborne (Andreas et al., 1995;Mayol et al., 2014). During dust periods (1D-Pr, 2D-Po, 3D-AA, 4D-Pr+Po, 5D-AA, 10D-Po, 17D-Po, 26D-Po, and 27D-AA), the size distribution of bacteria-associated particles generally showed two modes. During six cases of nondusty periods (9ND-Pr, 11ND-AA, 12ND-A, 13ND-A, 14ND-A, and 21ND-A), bacteria-associated particles mainly distributed in the size fraction 0.43–1.1 μm. In samples from the other nondusty periods (6ND-AA, 7ND-A, 8ND-A+Pr, 16ND-Po, 19ND-A, 20ND-A, 22ND-A, 23ND-Pr+Po, 24ND-Po+A, and 25ND-A), except for Samples 15ND-AA and 18ND-AA, bacteria-associated particles showed bimodal size distributions.

Table S1. Information of samplings. The sample ID indicates the sequence number (1 to 27) of the sample, and dust condition (D, dusty; ND, nondusty) and synoptic weather (Pr, prefront; Po, postfront; AA, approaching anticyclone; A, anticyclone) during the sampling period.

Sample ID	Year	Starting time (UTC+9:00)	Ending time (UTC+9:00)	Duration	Synoptic weather
1D-Pr	2013	19 Mar 22:50	20 Mar 03:00	04 h 10 min	Prefront
2D-Po		20 Mar 14:37	21 Mar 01:07	10 h 30 min	Postfront
3D-AA		21 Mar 06:00	21 Mar 18:00	12 h	Approaching anticyclone
4D-Pr+Po		14 Apr 23:55	15 Apr 09:02	09 h 07 min	Pre-/postfront
5D-AA		15 Apr 09:17	15 Apr 18:30	09 h 12 min	Approaching anticyclone
6ND-AA		27 Apr 00:00	28 Apr 00:00	24 h	Approaching anticyclone
7ND-A		28 Apr 00:01	29 Apr 00:01	24 h	Anticyclone
8ND-A+Pr		29 Apr 00:02	30 Apr 00:02	24 h	Anticyclone+prefront
9ND-Pr	2014	19 Mar 00:05	19 Mar 17:35	17 h 30 min	Prefront
10D-Po		20 Mar 12:00	21 Mar 12:00	24 h	Postfront
11ND-AA		21 Mar 12:00	22 Mar 12:10	24 h 10 min	Approaching anticyclone
12ND-A		23 Mar 12:40	24 Mar 12:40	24 h	Anticyclone
13ND-A		24 Mar 12:40	25 Mar 12:30	23 h 50 min	Anticyclone
14ND-A		25 Mar 12:30	25 Mar 19:45	07 h 15 min	Anticyclone
15ND-AA		27 Mar 11:23	28 Mar 08:40	21 h 27 min	Approaching anticyclone
16ND-Po	2015	20 Mar 18:10	21 Mar 18:10	24 h	Postfront
17D-AA		22 Mar 06:03	23 Mar 06:50	24 h 47 min	Approaching anticyclone
18ND-AA		23 Mar 07:58	24 Mar 08:00	24 h 02 min	Approaching anticyclone
19ND-A		24 Mar 08:03	25 Mar 08:02	23 h 59 min	Anticyclone
20ND-A		25 Mar 08:02	26 Mar 08:02	24 h	Anticyclone
21ND-A		26 Mar 08:05	27 Mar 07:30	23 h 25 min	Anticyclone
22ND-A	2016	22 Mar 09:04	23 Mar 09:02	23 h 58 min	Anticyclone
23ND-Pr+Po		23 Mar 09:00	24 Mar 09:00	24 h	Pre-/postfront
24ND-Po+A		24 Mar 09:00	25 Mar 09:00	24 h	Postfront/Anticyclone
25ND-A		25 Mar 09:00	26 Mar 07:00	22 h	Anticyclone
26D-Po		30 May 08:15	30 May 11:15	03 h	Postfront
27D-AA		31 May 07:50	31 May 10:50	03 h	Approaching anticyclone

Table S2. Data for Figures 1 and S9. Concentrations of viable (VB) and nonviable (NVB) bacteria (dC_B /dlog D_p, cells m^{-3}) and mineral dust-like particles (dC_M /dlog D_p, particles m^{-3}) in size-segregated airborne particles during the sampling periods.

Sample ID	Size range (μm) / Concentration	11-20	7-11	4.7-7	3.3-4.7	2.1-3.3	1.1-2.1	0.65-1.1	0.43-0.65
1D-Pr	130319NVB	1.9E+04	1.1E+05	1.7E+05	1.6E+05	7.5E+04	5.3E+04	5.3E+04	2.9E+04
	130319VB	2.8E+05	4.4E+05	8.9E+05	4.2E+05	3.7E+05	2.0E+05	2.9E+05	4.5E+05
2D-Po	130320NVB	8.3E+03	3.7E+04	3.5E+04	4.9E+04	1.1E+05	2.2E+04	1.6E+03	0.0E+00
	130320VB	8.0E+04	1.3E+05	1.1E+05	7.5E+04	1.5E+05	6.2E+04	8.6E+04	1.7E+05
3D-AA	130321NVB	7.6E+03	9.2E+03	1.0E+04	2.0E+04	2.4E+04	1.8E+04	1.9E+04	9.6E+03
	130321VB	8.3E+04	9.7E+04	7.5E+04	1.3E+05	2.0E+05	8.3E+04	1.1E+05	2.0E+05
4D-Pr+Po	130414NVB	1.0E+05	1.7E+05	2.4E+05	2.6E+05	2.5E+05	1.3E+05	1.5E+05	1.1E+05
	130414VB	2.5E+05	3.7E+05	3.5E+05	2.6E+05	3.0E+05	7.0E+04	2.3E+05	4.2E+05
5D-AA	130415NVB	5.6E+04	8.3E+04	2.0E+05	1.8E+05	1.9E+05	9.8E+04	4.6E+04	2.6E+04
	130415VB	1.5E+05	1.9E+05	2.6E+05	2.5E+05	1.6E+05	1.6E+05	1.2E+05	1.7E+05
6ND-AA	130427NVB	3.8E+04	1.9E+04	3.6E+04	3.7E+04	2.0E+04	1.3E+04	1.3E+04	1.1E+04
	130427VB	8.6E+04	5.3E+04	6.7E+04	8.5E+04	3.8E+04	4.5E+04	4.4E+04	1.4E+05
7ND-A	130428NVB	2.4E+04	1.8E+04	3.1E+04	2.9E+04	2.3E+04	1.2E+04	2.9E+04	2.1E+04
	130428VB	4.5E+04	5.0E+04	5.9E+04	6.4E+04	4.2E+04	4.2E+04	8.7E+04	1.5E+05
8ND-A+Pr	130429NVB	7.9E+03	2.3E+04	5.6E+04	5.1E+04	4.3E+04	2.0E+04	3.0E+04	2.8E+04
	130429VB	4.9E+04	5.4E+04	9.6E+04	8.8E+04	8.9E+04	5.4E+04	8.3E+04	1.4E+05
9ND-Pr	140319NVB	9.5E+03	2.1E+04	4.6E+04	3.2E+04	3.0E+04	5.8E+04	1.1E+05	3.2E+04
	140319VB	2.1E+04	0.0E+00	9.7E+03	6.4E+04	2.8E+03	6.1E+04	3.5E+05	4.5E+05
10D-Po	140320NVB	2.8E+04	6.0E+04	1.3E+05	2.5E+05	1.4E+05	5.9E+04	5.2E+04	6.9E+04
	140320VB	3.8E+04	9.5E+04	6.0E+02	1.8E+05	1.8E+04	5.2E+03	7.9E+04	1.1E+05
11ND-AA	140321NVB	1.0E+04	2.4E+04	3.3E+04	3.7E+03	5.2E+04	4.4E+04	6.0E+04	3.6E+04
	140321VB	3.1E+04	3.8E+04	2.8E+04	3.0E+04	4.5E+04	1.6E+04	1.2E+05	4.6E+05
12ND-A	140323NVB	2.1E+04	1.6E+04	6.3E+04	5.9E+03	3.0E+04	5.7E+04	3.1E+04	5.9E+03
	140323VB	4.3E+04	1.9E+04	4.5E+04	1.9E+04	2.5E+04	2.8E+04	3.1E+05	7.6E+05
13ND-A	140324NVB	4.1E+03	8.7E+04	2.0E+04	9.2E+04	5.3E+04	2.8E+04	1.1E+05	4.9E+04
	140324VB	2.7E+04	3.4E+04	0.0E+00	8.2E+04	6.3E+04	5.7E+04	3.9E+05	7.2E+05
14ND-A	140325NVB	1.6E+04	4.3E+04	7.1E+04	2.5E+04	3.0E+04	2.4E+04	0.0E+00	3.0E+03
	140325VB	0.0E+00	6.5E+04	7.7E+04	4.2E+04	6.1E+04	7.8E+04	0.0E+00	4.3E+05
15ND-AA	140327NVB	3.3E+04	4.7E+04	1.1E+05	1.3E+05	1.6E+05	1.0E+05	1.4E+05	4.1E+04
	140327VB	6.6E+05	6.6E+04	3.8E+04	4.4E+04	6.6E+04	4.5E+04	1.1E+05	2.1E+05
16ND-Po	150320NVB	9.2E+03	2.6E+04	2.1E+04	2.4E+04	2.6E+04	1.3E+04	1.3E+04	9.2E+02
	150320VB	1.3E+05	1.7E+05	2.0E+05	1.1E+05	8.4E+04	0.0E+00	2.5E+05	1.6E+05
17D-AA	150322Dust	7.3E+05	1.1E+06	2.9E+06	4.3E+06	2.8E+06	1.6E+06	5.7E+05	1.5E+05
	150322NVB	5.7E+04	6.1E+04	8.7E+04	9.4E+04	9.6E+04	6.8E+03	3.5E+03	0.0E+00
	150322VB	2.1E+04	5.2E+04	6.5E+04	1.6E+05	1.8E+05	7.9E+04	2.1E+05	3.0E+05
18ND-AA	150323Dust	1.2E+05	2.1E+05	7.3E+05	1.2E+06	7.9E+05	3.2E+05	5.8E+04	1.8E+04
	150323NVB	5.7E+03	1.1E+04	6.2E+03	5.3E+03	2.5E+04	2.6E+04	2.6E+04	7.3E+03
	150323VB	1.4E+05	1.6E+05	1.1E+05	3.7E+05	1.7E+05	1.4E+05	1.3E+05	8.4E+04
19ND-A	150324NVB	2.2E+04	2.0E+04	2.0E+04	3.2E+04	3.9E+04	9.9E+03	5.0E+03	9.2E+02
	150324VB	7.9E+03	0.0E+00	9.5E+03	7.7E+04	8.2E+04	3.1E+04	8.6E+04	8.8E+04
20ND-A	150325NVB	7.3E+03	5.4E+03	2.3E+04	2.8E+04	1.9E+04	5.3E+03	2.1E+04	7.8E+03
	150325VB	4.7E+03	3.0E+04	4.9E+04	8.9E+04	5.1E+04	1.1E+04	6.9E+04	1.0E+05
21ND-A	150326NVB	1.2E+04	3.7E+04	8.5E+04	4.4E+04	3.2E+04	4.5E+04	3.6E+04	1.7E+04
	150326VB	1.8E+04	0.0E+00	0.0E+00	4.2E+04	0.0E+00	0.0E+00	1.5E+04	5.0E+05
22ND-A	160322Dust	1.5E+04	2.4E+04	7.2E+04	1.4E+05	1.6E+05	1.1E+05	9.3E+04	3.3E+04
	160322NVB	3.5E+03	2.5E+03	3.9E+04	7.5E+04	8.3E+04	4.9E+04	7.4E+04	3.5E+04
	160322VB	0.0E+00	3.1E+04	3.3E+04	2.6E+04	1.1E+04	4.1E+03	6.3E+04	8.3E+04
23ND-Pr+Po	160323Dust	1.8E+04	8.1E+04	3.5E+04	1.6E+05	2.8E+05	2.1E+05	6.1E+04	3.2E+03
	160323NVB	6.0E+03	1.3E+04	0.0E+00	3.2E+04	7.2E+04	5.1E+04	1.9E+04	9.2E+03
	160323VB	4.1E+03	2.2E+04	2.8E+03	5.3E+03	1.8E+04	2.7E+04	9.7E+04	1.3E+05
24ND-Po+A	160324Dust	5.6E+04	9.2E+03	2.0E+05	2.6E+05	1.6E+05	1.0E+05	6.2E+04	6.9E+03
	160324NVB	6.6E+03	3.3E+03	5.1E+04	7.4E+04	1.9E+04	2.0E+04	2.3E+04	4.6E+03
	160324VB	3.4E+04	6.5E+04	7.8E+04	2.9E+04	8.4E+02	4.5E+04	1.3E+05	8.5E+04
25ND-A	160325Dust	2.4E+04	4.9E+04	1.5E+05	1.9E+05	1.9E+05	1.3E+05	5.8E+04	4.5E+04
	160325NVB	5.9E+03	4.6E+03	1.7E+04	1.2E+04	3.1E+04	2.4E+04	1.1E+04	3.5E+03
	160325VB	4.5E+04	1.4E+05	3.9E+04	3.1E+04	3.7E+04	4.5E+04	1.2E+05	1.7E+05
26D-Po	160530Dust	1.2E+05	1.6E+05	1.8E+05	3.4E+05	3.2E+05	3.8E+05	1.6E+05	6.6E+04
	160530NVB	1.8E+04	3.7E+04	4.2E+04	1.7E+04	2.0E+04	1.6E+04	2.9E+04	3.7E+03
	160530VB	1.8E+05	8.3E+05	3.6E+05	3.2E+05	6.1E+05	3.6E+05	4.9E+05	7.1E+05
27D-AA	160531Dust	7.8E+04	1.7E+05	4.3E+05	2.2E+05	5.3E+05	3.7E+05	1.2E+05	1.8E+04
	160531NVB	5.1E+03	2.7E+04	1.9E+04	1.3E+04	1.3E+04	2.6E+04	5.8E+03	1.1E+04
	160531VB	5.1E+04	2.6E+05	0.0E+00	0.0E+00	0.0E+00	4.9E+04	2.3E+05	1.8E+05

Table S3. Data for Figure 2. Concentrations of viable (VB), nonviable (NVB), and total (TB) bacteria (C_B, cells m^{-3}) and mineral dust-like particles (C_M, particles m^{-3}) in size-segregated airborne particles.

Sample ID \ Size range (μm) / Concentration		11-20	7-11	4.7-7	3.3-4.7	2.1-3.3	1.1-2.1	0.65-1.1	0.43-0.65
17D-AA	150322Dust	1.9E+05	2.1E+05	5.1E+05	6.6E+05	5.5E+05	4.6E+05	1.3E+05	2.7E+04
	150322VB	5.3E+03	1.0E+04	1.1E+04	2.5E+04	3.5E+04	2.2E+04	4.9E+04	5.4E+04
	150322NVB	1.5E+04	1.2E+04	1.5E+04	1.4E+04	1.9E+04	1.9E+03	8.0E+02	0.0E+00
	150322TB	2.0E+04	2.2E+04	2.6E+04	3.9E+04	5.4E+04	2.4E+04	5.0E+04	5.4E+04
18ND-AA	150323Dust	3.1E+04	4.1E+04	1.3E+05	1.9E+05	1.5E+05	9.1E+04	1.3E+04	3.2E+03
	150323VB	3.6E+04	3.2E+04	2.0E+04	5.6E+04	3.4E+04	4.0E+04	3.0E+04	1.5E+04
	150323NVB	1.5E+03	2.2E+03	1.1E+03	8.2E+02	5.0E+03	7.2E+03	5.9E+03	1.3E+03
	150323TB	3.8E+04	3.4E+04	2.1E+04	5.7E+04	3.9E+04	4.7E+04	3.6E+04	1.6E+04
22ND-A	160322Dust	3.9E+03	4.7E+03	1.2E+04	2.2E+04	3.1E+04	3.1E+04	2.1E+04	6.0E+03
	160322VB	0.0E+00	6.2E+03	5.7E+03	3.9E+03	2.2E+03	1.2E+03	1.4E+04	1.5E+04
	160322NVB	9.0E+02	4.9E+02	6.7E+03	1.2E+04	1.6E+04	1.4E+04	1.7E+04	6.3E+03
	160322TB	9.0E+02	6.7E+03	1.2E+04	1.6E+04	1.9E+04	1.5E+04	3.1E+04	2.1E+04
23ND-Pr+Po	160323Dust	4.8E+03	1.6E+04	6.1E+03	2.4E+04	5.4E+04	5.9E+04	1.4E+04	5.7E+02
	160323VB	1.1E+03	4.4E+03	4.9E+02	8.2E+02	3.6E+03	7.6E+03	2.2E+04	2.2E+04
	160323NVB	1.6E+03	2.5E+03	0.0E+00	4.8E+03	1.4E+04	1.4E+04	4.4E+03	1.6E+03
	160323TB	2.6E+03	6.9E+03	4.9E+02	5.7E+03	1.8E+04	2.2E+04	2.7E+04	2.4E+04
24ND-Po+A	160324Dust	1.4E+04	1.8E+03	3.4E+04	4.0E+04	3.1E+04	2.9E+04	1.4E+04	1.2E+03
	160324VB	8.8E+03	1.3E+04	1.3E+04	4.5E+03	1.6E+02	1.3E+04	3.0E+04	1.5E+04
	160324NVB	1.7E+03	6.6E+02	8.8E+03	1.1E+04	3.7E+03	5.6E+03	5.2E+03	8.2E+02
	160324TB	1.1E+04	1.3E+04	2.2E+04	1.6E+04	3.9E+03	1.8E+04	3.6E+04	1.6E+04
25ND-A	160325Dust	6.4E+03	9.7E+03	2.7E+04	2.9E+04	3.8E+04	3.8E+04	1.3E+04	8.2E+03
	160325VB	1.2E+04	2.8E+04	6.8E+03	4.7E+03	7.3E+03	1.3E+04	2.7E+04	3.0E+04
	160325NVB	1.5E+03	9.0E+02	2.9E+03	1.9E+03	6.1E+03	6.6E+03	2.4E+03	6.3E+02
	160325TB	1.3E+04	2.8E+04	9.7E+03	6.6E+03	1.3E+04	1.9E+04	3.0E+04	3.1E+04
26D-Po	160530Dust	3.1E+04	3.1E+04	3.2E+04	5.2E+04	6.2E+04	1.1E+05	3.5E+04	1.2E+04
	160530VB	4.8E+04	1.6E+05	6.2E+04	4.9E+04	1.2E+05	1.0E+05	1.1E+05	1.3E+05
	160530NVB	4.6E+03	7.2E+03	7.2E+03	2.6E+03	3.9E+03	4.6E+03	6.6E+03	6.6E+02
	160530TB	5.3E+04	1.7E+05	7.0E+04	5.1E+04	1.2E+05	1.1E+05	1.2E+05	1.3E+05
27D-AA	160531Dust	2.0E+04	3.4E+04	7.4E+04	3.4E+04	1.0E+05	1.0E+05	2.8E+04	3.3E+03
	160531VB	1.3E+04	5.1E+04	0.0E+00	0.0E+00	0.0E+00	1.4E+04	5.2E+04	3.2E+04
	160531NVB	1.3E+03	5.3E+03	3.3E+03	2.0E+03	2.6E+03	7.2E+03	1.3E+03	2.0E+03
	160531TB	1.4E+04	5.6E+04	3.3E+03	2.0E+03	2.6E+03	2.1E+04	5.3E+04	3.4E+04

References

Andreas, E. L., Edson, J. B., Monahan, E. C., Rouault, M. P., and Smith, S. D.: The spray contribution to net evaporation from the sea: A review of recent progress, Boundary-Layer Meteorology, 72, 3-52, https://doi.org/10.1007/BF00712389, 1995.

Bakken, L. R., and Olsen, R. A.: Buoyant densities and dry-matter contents of microorganisms: conversion of a measured biovolume into biomass, Appl. Environ. Microbiol., 45, 1188-1195, 1983.

Bratbak, G., and Dundas, I.: Bacterial dry matter content and biomass estimations, Applied & Environmental Microbiology, 48, 755-757, 1984.

Hara, K., Zhang, D., Yamada, M., Matsusaki, H., and Arizono, K.: A detection of airborne particles carrying viable bacteria in an urban atmosphere of Japan, Asian J. Atmos. Environ., 5, 152-156, 10.5572/ajae.2011.5.3.152, 2011.

Hu, W., Murata, K., Fukuyama, S., Kawai, Y., Oka, E., Uematsu, M., and Zhang, D.: Concentration and Viability of Airborne Bacteria Over the Kuroshio Extension Region in the Northwestern Pacific Ocean: Data From Three Cruises, J. Geophys. Res. Atmos., 122, 12892-12905, 10.1002/2017jd027287, 2017.

Huffman, J. A., Sinha, B., Garland, R. M., Snee-Pollmann, A., Gunthe, S. S., Artaxo, P., Martin, S. T., Andreae, M. O., and Pöschl, U.: Size distributions and temporal variations of biological aerosol particles in the Amazon rainforest characterized by microscopy and real-time UV-APS fluorescence techniques during AMAZE-08, Atmos. Chem. Phys., 12, 11997-12019, 10.5194/acp-12-11997-2012, 2012.

Mayol, E., Jimenez, M. A., Herndl, G. J., Duarte, C. M., and Arrieta, J. M.: Resolving the abundance and air-sea fluxes of airborne microorganisms in the North Atlantic Ocean, Front. Microbiol., 5, 557, 10.3389/fmicb.2014.00557, 2014.

Murata, K., and Zhang, D.: Applicability of LIVE/DEAD BacLight stain with glutaraldehyde fixation for the measurement of bacterial cell concentration and viability in the air, Aerosol Air Qual. Res., 13, 1755-1767, 10.4209/aaqr.2012.10.0293, 2013.

Murata, K., and Zhang, D.: Concentration of bacterial aerosols in response to synoptic weather and land-sea breeze at a seaside site downwind of the Asian continent, J. Geophys. Res. Atmos., 121, 11636-11647, 10.1002/2016jd025028, 2016.